Наносистеми, наноматеріали, нанотехнології
Nanosistemi, Nanomateriali, Nanotehnologii
2024, т. 22, № 1, сс. 1–11
https://doi.org/10.15407/nnn.22.01.001

PACS numbers: 61.72.Cc, 61.72.Mm, 68.35.Ct, 68.37.Ps, 68.55. A-, 68.55. Jk, 81.15.Cd

Surface Morphology of Thin Films of $(Y_{0.06}Ga_{0.94})_2O_3$ Activated by Cr^{3+}

O. M. Bordun[1], B. O. Bordun[1], I. I. Medvid[1], M. V. Protsak[1], I. Yo. Kukharskyy[1], K. L. Biliak[1], D. M. Maksymchuk[1], I. M. Kofliuk[1], and D. S. Leonov[2]

[1]*Ivan Franko National University of Lviv,*
50, Drahomanov Str.,
UA-79005 Lviv, Ukraine
[2]*Technical Centre, N.A.S. of Ukraine,*
13, Pokrovska Str.,
UA-04070 Kyiv, Ukraine

Thin films of $(Y_{0.06}Ga_{0.94})_2O_3$:Cr are obtained by radio-frequency (RF) ion-plasma sputtering in an argon atmosphere on polycrystalline polycor and amorphous υ-SiO_2 substrates. The study of the surface morphology of thin films by atomic force microscopy (AFM) shows that the transition from υ-SiO_2 substrates to polycor increases the average diameter of crystallites, which form the film, from 123 nm to 372 nm for films annealed in an argon atmosphere. The heat treatment of films on υ-SiO_2 substrates in an argon atmosphere leads to an increase in the root-mean-square roughness of thin films, which is of 1.2 nm and 2.9 nm for the unannealed and annealed films in an argon atmosphere, respectively. The analysis of the distributions of crystallites by the value of the grain diameter is carried out, and, as found during the heat treatment of $(Y_{0.06}Ga_{0.94})_2O_3$:Cr films on υ-SiO_2 substrates, the growth of crystallites perpendicular to the film surface is observed.

Методом високочастотного (ВЧ) йонно-плазмового розпорошення в атмосфері арґону на полікристалічних підкладинках полікору й аморфних підкладинках υ-SiO_2 одержано тонкі плівки $(Y_{0,06}Ga_{0,94})_2O_3$:Cr. Дослідження морфології поверхні тонких плівок методом атомно-силової мікроскопії (АСМ) показали, що з переходом від підкладинок υ-SiO_2 до полікору зростає середній діяметер кристалітів, які формують плівку від 123 нм до 372 нм для плівок, відпалених у атмосфері арґону. Термооброблення плівок на підкладинках з υ-SiO_2 у атмосфері арґону приводить до збільшення середньоквадратичної шерсткости тонких плівок, що становлять для невідпаленої та відпаленої плівок у атмосфері арґону 1,2 нм і 2,9 нм відповідно. Проведено аналізу розподілів кристалітів за величиною діяметра зерен і встановлено, що за термооброблення плівок $(Y_{0.06}Ga_{0.94})_2O_3$:Cr на підкладинках υ-SiO_2 спостерігається зростання кри-

сталітів перпендикулярно до поверхні плівки.

Key words: gallium oxide, chromium activator, thin films, crystallites, surface morphology, AFM.

Ключові слова: оксид Ґалію, хром-активатор, тонкі плівки, кристаліти, морфологія поверхні, АСМ.

(Received 21 December, 2023)

1. INTRODUCTION

In recent years, nanostructured oxide materials have been widely studied, among which Ga_2O_3 occupies an important place. Gallium oxide β-Ga_2O_3 belongs to the wide-bandgap semiconductors, with a bandgap width of 4.5 to 5.1 eV, depending on the preparation conditions. This material is widely used in solar cells, gas sensors, ultraviolet photodetectors, luminescent devices, high-power Schottky diodes, and transistors [1–10]. Due to its good chemical and thermal stability, this material is promising for use in luminescent devices. In this regard, pure gallium oxide thin films, activated by various impurities, obtained by various methods, are widely studied. The photoluminescence spectrum of gallium oxide at room temperature usually shows ultraviolet and blue radiation [11–15]. In general, the optical and electrical characteristics of thin films based on β-Ga_2O_3 are determined by the methods of their preparation, deposition modes, substrate type, and processing technology, as well as the introduction of impurities, which can purposefully change the spectral-luminescent and electrophysical properties of these films. To this end, thin films with the chemical composition $(Y_{0.06}Ga_{0.94})_2O_3$:Cr were studied in this work, in which some Ga^{3+} ions were replaced by isovalent Y^{3+} ions, which did not require local compensation of the electric charge. This substitution is because Y_2O_3 films are also quite promising in terms of their use in modern optoelectronic and luminescent technology [16–19]. This also allows us to better study the luminescence centres in thin films based on β-Ga_2O_3 since the luminescence efficiency in these films is largely determined by the peculiarities of recombination processes, which luminescence centres of defective origin usually cause.

In general, the physical properties of thin films are complicated because films do not always have a perfect structure and can be polycrystalline, amorphous, and contain inclusions of other phases. Obtaining the required and stable reproducible properties of polycrystalline films is further complicated by the presence of intergranular boundaries (IGBs). The physical properties of polycrystalline thin films are largely determined not only by the material properties but also by the energy

levels arising from the presence of the IGBs. It is clear that such levels are also determined by the size of the crystallites that form the thin films. This led to the study of the surface morphology of thin films of $(Y_{0.06}Ga_{0.94})_2O_3$:Cr using atomic force microscopy, which is presented in this paper. The films were obtained by the method of RF ion-plasma sputtering, which is optimal for obtaining homogeneous semiconductor and dielectric films [19].

2. EXPERIMENTAL TECHNIQUE

Thin films of $(Y_{0.06}Ga_{0.94})_2O_3$:Cr with a thickness of 0.5–1.2 μm were obtained by RF ion-plasma sputtering on polycrystalline polycor ((99.8% α(alpha)-Al_2O_3) substrates and amorphous fused quartz υ-SiO_2 substrates. The RF sputtering was carried out in an argon atmosphere in a system using the magnetic field of external solenoids for compression and additional ionization of the plasma column. The feedstock was a mixture of Y_2O_3 and Ga_2O_3 oxides of the stoichiometric composition of the 'ОСЧ' grade (extra pure). The concentration of the Cr^{3+} activator was 0.5 mol.%. After the films were deposited on υ-SiO_2 and polycor substrates, they were heat treated in argon at 1000–1100°C.

The structure and phase composition of the obtained films were studied by x-ray diffraction analysis (Shimadzu XDR-600). X-ray diffraction studies showed the presence of a polycrystalline structure with a predominant orientation in the (002), (111), (110), and (512) planes. The analysis of the obtained diffractograms shows that the structure of the films obtained corresponds to the monoclinic crystal structure of β-Ga_2O_3. The diffractograms of $(Y_{0.06}Ga_{0.94})_2O_3$:Cr thin films almost completely correspond to the diffractograms of unalloyed $(Y_{0.06}Ga_{0.94})_2O_3$ thin films, which were presented earlier in our work [20].

The surface morphology of the films was studied using an INTEGRA TS-150 atomic force microscope (AFM). The image of the surface of thin films was obtained in the semi-contact mode.

The x-ray photoelectron spectroscopy (XPS) method was used to analyse the elemental composition of the surface of the obtained thin films. The x-ray photoelectron spectroscopy (XPS, Phoibos 150, Specs) spectra were recorded using a monochromatic x-ray source AlK_α (1486.6 eV). The binding energy was calibrated against the signal from C1*s* at 285.0 eV.

3. RESULTS AND DISCUSSION

Microphotographs of the surface of $(Y_{0.06}Ga_{0.94})_2O_3$:Cr thin films obtained by RF ion plasma sputtering on υ-SiO_2 substrates without

heat treatment and after heat treatment in an argon atmosphere and on polycor substrates after heat treatment in an argon atmosphere are shown in Fig. 1.

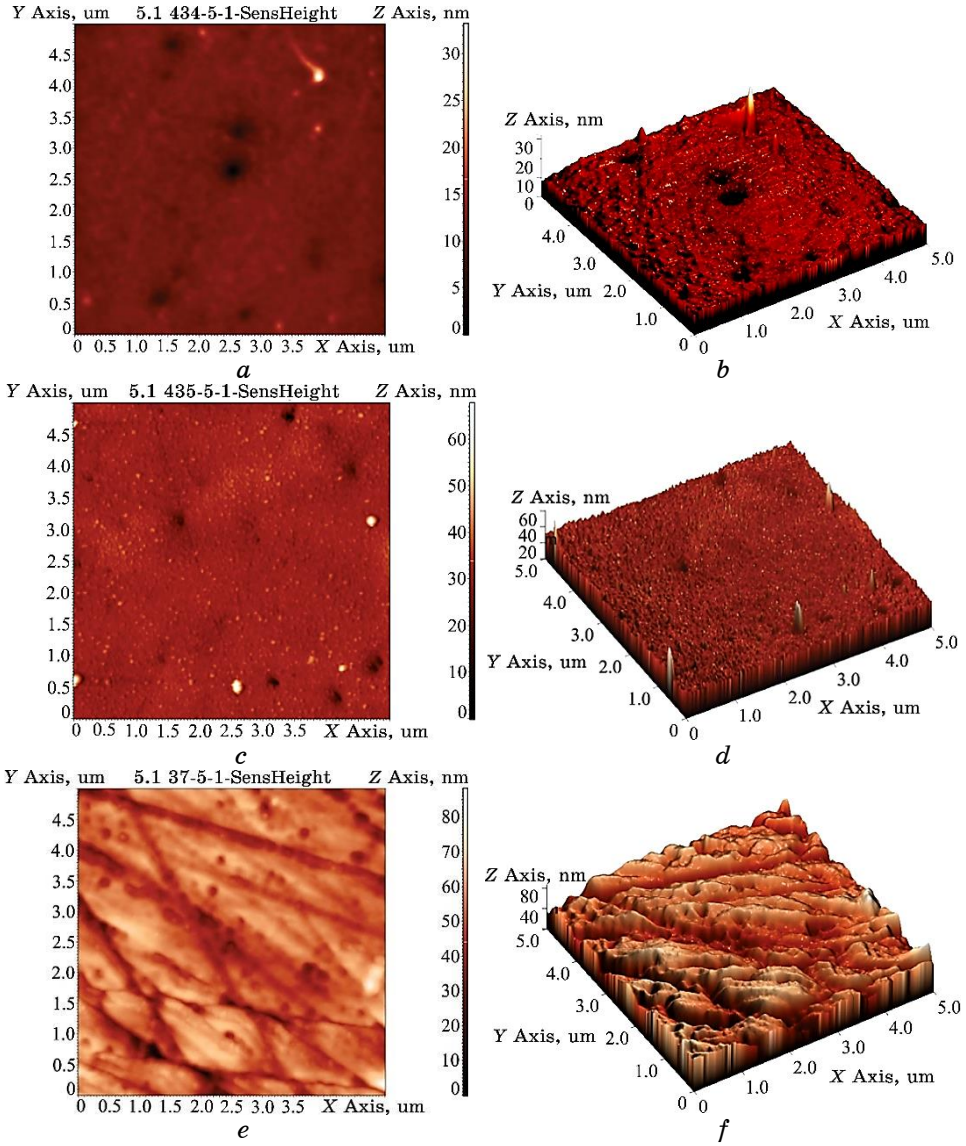

Fig. 1. Images of the surface morphology of $(Y_{0.06}Ga_{0.94})_2O_3$:Cr thin films obtained by RF sputtering on υ-SiO_2 substrates without heat treatment (*a*, *b*) and after heat treatment in an argon atmosphere (*c*, *d*) and on polycor substrates after heat treatment in an argon atmosphere (*e*, *f*). Images *a*, *c* and *e* are two-dimensional, *b*, *d* and *f* are three-dimensional.

TABLE. Parameters of crystal grains of thin films of $(Y_{0.06}Ga_{0.94})_2O_3$:Cr.

Parameter	Without heat treatment on υ-SiO_2 substrate	Heat treatment in Ar on a υ-SiO_2 substrate	Heat treatment in Ar on a polycor substrate
Average grain diameter, nm	181	123	372
RMS roughness, nm	1,2	2,9	9,5
Maximum grain height, nm	12	33	55
Average grain volume, nm^3	2960	6040	234000

The topography of the samples was quantitatively characterized by standard parameters: root-mean-square roughness, maximum grain height, average grain diameter, and average grain volume, which were calculated from AFM data using the Image Analysis 3.5 image-processing module for areas of the same size (5000×5000 nm).

The characteristic parameters of $(Y_{0.06}Ga_{0.94})_2O_3$:Cr thin films deposited on υ-SiO_2 substrates without heat treatment and for films deposited on υ-SiO_2 and polycor substrates after heat treatment in an argon atmosphere are shown in Table.

As can be seen from the results obtained, different types of substrates and the presence of heat treatment have a significant effect on the size of crystal grains and surface roughness of the obtained samples.

The analysis of AFM images (Fig. 1) and parameters of crystal grains (Table) of the surface of $(Y_{0.06}Ga_{0.94})_2O_3$:Cr films shows that the films deposited on the amorphous quartz substrate υ-SiO_2 are formed from significantly smaller grains than when the films are deposited on a polycrystalline polycor substrate. The size of crystallites of thin films of $(Y_{0.06}Ga_{0.94})_2O_3$:Cr deposited on a υ-SiO_2 substrate after heat treatment in an argon atmosphere increases, although a decrease in the average size of the diameter of the grains, from which these films are formed is observed. At the same time, the value of the average volume of crystallites increases significantly. Such an increase in the size of crystalline grains and, in particular, an increase in the average grain volume and changes in the value of the root-mean-square roughness indicate a complication of the surface structure.

A comparison of the histograms of the distribution of grain heights (Fig. 2) shows that smaller grains are formed on fused quartz substrates, which form the surface of unannealed $(Y_{0.06}Ga_{0.94})_2O_3$:Cr thin films, although their average diameters are

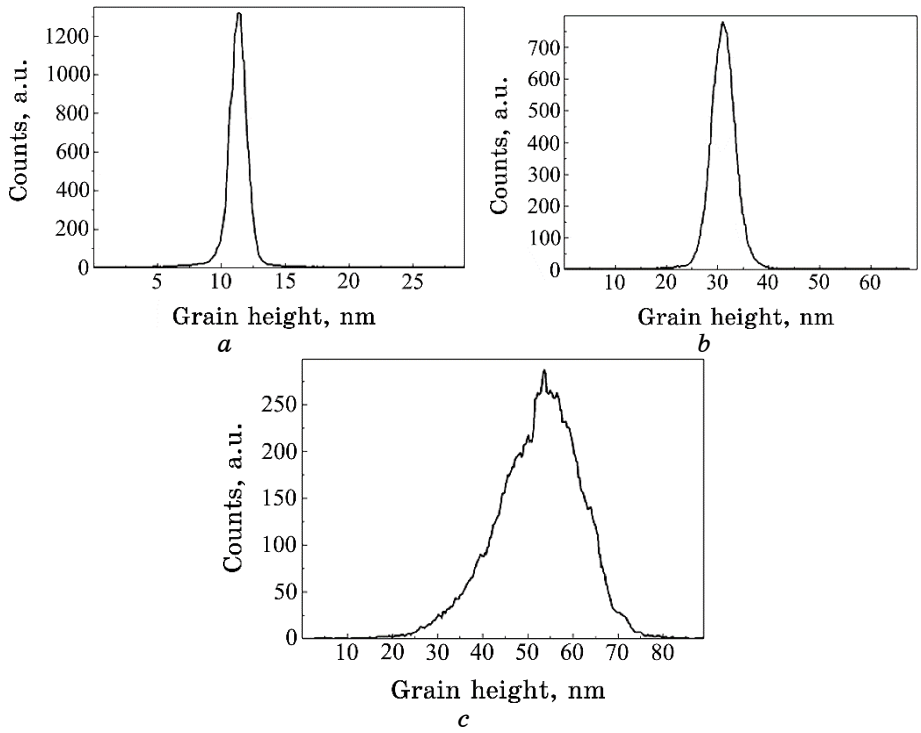

Fig. 2. Distribution of grain heights for AFM images of $(Y_{0.06}Ga_{0.94})_2O_3$:Cr thin films obtained by RF sputtering on υ-SiO_2 substrates without heat treatment (*a*), after heat treatment in an argon atmosphere (*b*), and on polycor substrates after heat treatment in an argon atmosphere (*c*).

larger than those of annealed films in an argon atmosphere are. Heat treatment of thin films of $(Y_{0.06}Ga_{0.94})_2O_3$:Cr deposited on a quartz substrate in an argon atmosphere significantly affects the value of grain height compared to unannealed films (increases by about 2.4 times). If we compare the parameter RMS surface roughness of thin films, then, for films deposited on NaCl substrates, it is the highest value compared to unannealed films and films subjected to heat treatment in an argon atmosphere deposited on quartz substrates. For films annealed in an argon atmosphere and deposited on polycor substrates, the value of this parameter differs by about 3.3 times compared to thin films of $(Y_{0.06}Ga_{0.94})_2O_3$:Cr deposited on a quartz substrate.

The increase in the size of crystalline grains in $(Y_{0.06}Ga_{0.94})_2O_3$:Cr thin films after heat treatment (Table) indicates the possibility of the transition of the film surface to a more nanostructured state due to the crystallization of the surface layer.

The characteristic distributions of grain diameter sizes in thin films of $(Y_{0.06}Ga_{0.94})_2O_3$:Cr depending on the type of substrate and the presence of heat treatment are shown in Fig. 3.

A thorough review [21] analysed the growth of crystal grains in thin films and the evolution of crystal structures and showed that polycrystalline thin films with thicknesses up to 1 μm, which is typical for our $(Y_{0.06}Ga_{0.94})_2O_3$:Cr films, often have 2*D*-like structures. In such structures, most grain boundaries are perpendicular to the film surface. Most of the materials analysed in [21] form films of nonequilibrium grains with sizes smaller than the film thickness and form two-dimensional structures only after annealing. Based on numerical results, [21] also concluded that the formation of grains in thin films is difficult to describe accurately using modelling or comparison with experiments that described the study of foams or monolayers. In general, grain sizes in polycrystalline films are lognormally distributed in size.

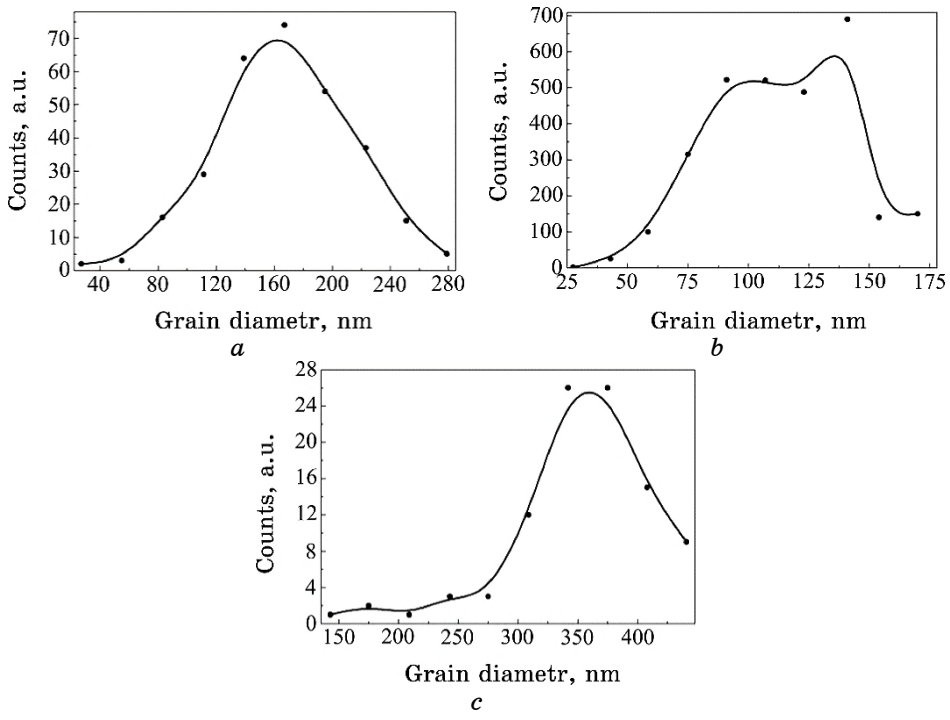

Fig. 3. The distribution of grain diameter sizes and the calculated approximate diameter distribution on AFM images of $(Y_{0.06}Ga_{0.94})_2O_3$:Cr thin films obtained by RF sputtering on υ-SiO_2 substrates without heat treatment (*a*), after heat treatment in an argon atmosphere (*b*), and on polycor substrates after heat treatment in an argon atmosphere (*c*).

In some cases, further grain growth is observed due to 'anomalous' growth or preferential growth of several grains, which usually have specific crystallographic orientation relations relative to the substrate surface plane. Our results show that such a situation is most likely characteristic of the $(Y_{0.06}Ga_{0.94})_2O_3$:Cr films we obtained. When the number of growing grains leads to a 'matrix' of grains beyond the static boundaries, a bimodal grain size distribution develops, which is called secondary grain growth [22]. Grains that grow abnormally often have a limited or homogeneous texture. Secondary grain growth in thin films typically involves an evolution in the distribution of grain textures as well as an evolution in the grain size distribution.

Our results of the distribution of grain diameter sizes in thin films of $(Y_{0.06}Ga_{0.94})_2O_3$:Cr (Fig. 3) indicate that when these films are deposited on polycor substrates after annealing in an argon atmosphere, an unimodal distribution of diameters with a maximum in the region of 365 nm is observed. A more complex shape of the diameter distribution is formed when the films are deposited on an amorphous υ-SiO_2 substrate after annealing in an argon atmosphere. In particular, for freshly deposited films (Fig. 3, *a*), a unimodal distribution with a maximum in the 170 nm region is manifested. After heat treatment of such films in an argon atmosphere (Fig. 3, *b*), a bimodal distribution with maxima in the region of 100 and 135 nm is observed.

Analysing the situation described above, we can conclude that during the heat treatment process, grain growth occurs due to the processes of growth and sintering. It should be noted that a similar situation is observed during RF deposition on υ-SiO_2 substrates and β-Ga_2O_3 thin films, where the growth of secondary and tertiary grains is observed [23]. The growth of secondary and even tertiary grains was observed in these films both during RF sputtering and during heat treatment.

For unannealed $(Y_{0.06}Ga_{0.94})_2O_3$:Cr thin films deposited on υ-SiO_2 substrates and annealed films in an argon atmosphere deposited on polycor substrates, the distribution of grains by diameter is well described by a normal logarithmic law. This situation is typical for the distribution of grains by diameter in polycrystalline films [24]. In particular, this situation is observed during the RF deposition of Y_2O_3:Eu thin films [25].

To describe the obtained dependences (Fig. 3, *a*, *c*), we use the normal logarithmic law, which is used to distribute grains by diameter size in polycrystalline films [24]:

$$f(D) = \frac{1}{\sigma D\sqrt{2\pi}} \exp\left[-\frac{(\ln D - \mu)^2}{2\sigma^2}\right],$$

where $\int_0^\infty f(x)dx = 1$, D is the grain diameter divided by the film thickness; μ is the average value of $\ln D$; σ is the standard deviation (dispersion) of $\ln D - \mu$. When fitting the data, μ and σ are independent adjustable parameters.

Our analysis shows that during the RF deposition of thin films on a υ-SiO_2 substrate, a unimodal distribution of grains in terms of diameter is observed (Fig. 3, *a*) with a maximum at 170 nm and a dispersion of 6.2 nm. The subsequent annealing of these films in an argon atmosphere results in a bimodal distribution of overlapping bands with maxima located in regions around 100 and 135 nm. Due to the significant overlap, the variances of these distributions are 25.1 and 13.3 nm, respectively. It is characteristic that grain growth during the annealing of thin films of $(Y_{0.06}Ga_{0.94})_2O_3$:Cr occurs in the direction perpendicular to the film surface. During the annealing of $(Y_{0.06}Ga_{0.94})_2O_3$:Cr films deposited on a polycor substrate, an unimodal lognormal distribution of grain diameter sizes with a maximum in the region of 365 nm and a dispersion of 2.7 nm is observed.

To verify the elemental composition of the obtained thin films, x-ray photoelectron spectroscopy (XPS) spectra were analysed. The characteristic XPS spectra for the unannealed $(Y_{0.06}Ga_{0.94})_2O_3$:Cr thin films deposited on υ-SiO_2 substrates and the annealed films in the argon atmosphere deposited on υ-SiO_2 and polycor substrates are shown in Fig. 4.

The analysis showed that the recorded spectra contain peaks corresponding to O1*s*, C1*s*, Y3*d*, Ga3*p*, and Cr2*p* atoms. At the same

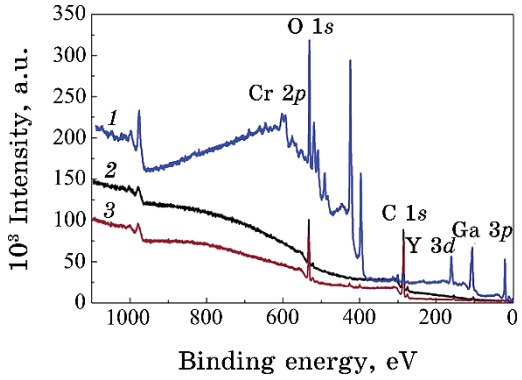

Fig. 4. XPS spectra of $(Y_{0.06}Ga_{0.94})_2O_3$:Cr thin films obtained by RF sputtering on υ-SiO_2 substrates without heat treatment (*1*), after heat treatment in an argon atmosphere (*2*), and on polycor substrates after heat treatment in an argon atmosphere (*3*).

time, the peak characteristic of the Cr 2*p* atom is expressed relatively weakly, since the chromium concentration in the obtained films is insignificant. It is characteristic that it is most intensively manifested in $(Y_{0.06}Ga_{0.94})_2O_3$:Cr films deposited on polycor substrates.

4. CONCLUSIONS

It has been established that thin films of $(Y_{0.06}Ga_{0.94})_2O_3$:Cr formed from nanometer grains are formed by RF ion-plasma sputtering on polycrystalline polycor and amorphous υ-SiO_2 substrates. Based on the AFM images, it is shown that the average diameters of the crystallites of the films on polycor substrates after heat treatment in an argon atmosphere are of 372 nm, on υ-SiO_2 substrates without heat treatment, are of 181 nm, and after heat treatment in an argon atmosphere, are of 123 nm. The heat treatment of films on υ-SiO_2 substrates in an argon atmosphere leads to an increase in the root mean square roughness from 1.2 to 2.9 nm. It has been found that when thin films of $(Y_{0.06}Ga_{0.94})_2O_3$:Cr are deposited on υ-SiO_2 substrates, an unimodal lognormal distribution of grains in terms of diameter size with a maximum at 170 nm and a dispersion of 6.2 nm is observed. In the process of heat treatment of such films, a bimodal distribution appears with maxima at 100 and 135 nm and dispersions of 25.1 and 13 nm, respectively. During this heat treatment, grain growth perpendicular to the film surface is observed. During the heat treatment of films deposited on polycarbonate substrates, a unimodal distribution of grains by diameter with a maximum of 365 nm and a dispersion of 2.7 nm occurs.

REFERENCES

1. M. Higashiwaki, K. Sasaki, A. Kuramata, T. Masui and S. Yamakoshi, *phys. status solidi (a)*, **211**, No. 1: 21 (2014); https://doi.org/10.1002/pssa.201330197
2. M. He, Q. Zeng, and L. Ye, Crystals, **13**, No. 10: 1434 (2023); https://doi.org/10.3390/cryst13101434
3. X. Chen, K. W. Liu, Z. Z. Zhang, C. R. Wang, B. H. Li, H. F. Zhao, D. X. Zhao, and D. Z. Shen, *ACS Appl. Mater. Inter.*, **8**, No. 6: 4185 (2016); https://doi.org/10.1021/acsami.5b11956
4. S. Kumar and R. Singh, *phys. status solidi (RRL)*, **7**, No. 10: 781 (2013); https://doi.org/10.1002/pssr.201307253
5. D. Y. Guo, Z. P. Wu, Y. H. An, P. G. Li, P. C. Wang, X. L. Chu, X. C. Guo, Y. S. Zhi, M. Lei, L. H. Li, and W. H. Tang, *Appl. Phys. Lett.*, **106**, No. 6: 042105 (2015); https://doi.org/10.1063/1.4907174
6. S. Kumar, S. Dhara, R. Agarwal, and R. Singh, *J. Alloys Compounds*, **683**: 143 (2016); https://doi.org/10.1016/j.jallcom.2016.05.079

7. R. Suzuki, S. Nakagomi, Y. Kokubun, N. Arai, and S. Ohira, *Appl. Phys. Lett.*, **94**, No. 22: 222102 (2009); https://doi.org/10.1063/1.3147197
8. K. Sasaki, M. Higashiwaki, A. Kuramata, T. Masui, and S. Yamakoshi, *IEEE Electron. Device Lett.*, **34**, No. 4: 493 (2013); https://doi.org10.1109/LED.2013.2244057
9. M. Higashiwaki, *AAPPS Bull.*, **32**: 3 (2022); https://doi.org/10.1007/s43673-021-00033-0
10. K. Sasaki, M. Higashiwaki, A. Kuramata, T. Masui, and S. Yamakoshi, *J. Cryst. Growth*, **378**: 591 (2013); https://doi.org/10.1016/j.jcrysgro.2013.02.015
11. O. M. Bordun, B. O. Bordun, I. Yo. Kukharskyy, and I. I. Medvid, *J. Appl. Spectrosc.*, **86**, No. 6: 1010 (2020); https://doi.org/10.1007/s10812-020-00932-4
12. A. K. Saikumar, Sh. D. Nehate, and K. B. Sundaram, *ECS J. of Solid State Science and Technol.*, **8**, No. 7: Q3064 (2019); https://doi.org/10.1149/2.0141907jss
13. Lingyi Kong, Jin Ma, Caina Luan, Wei Mi, and Yu Lv, *Thin Solid Films*, **520**, No. 13: 4270 (2012); https://doi.org/10.1016/j.tsf.2012.02.027
14. O. M. Bordun, B. O. Bordun, I. I. Medvid, and I. Yo. Kukharskyy, *Acta Physica Polonica A*, **133**, No. 4: 910 (2018); https://doi.org/10.12693/APhysPolA.133.910
15. K. H. Choi and H. C. Kang, *Materials Letters*, **123**: 160 (2014); https://doi.org/10.1016/j.matlet.2014.03.038
16. C. B. Willingham, J. M. Wahl, P. K. Hogan, L. C. Kupferberg, T. Y. Wong, and A. M. De, *Proc. SPIE*, **5078**: 179 (2003); https://doi.org/10.1117/12.500986
17. T. Igarashi, M. Ihara, T. Kusunoki, K. Ohno, T. Isobe, and M. Senna, *Appl. Phys. Lett.*, **76**, No. 12: 1549 (2000); https://doi.org/10.1063/1.1260921
18. O. M. Bordun, I. M. Bordun, and S. S. Novosad, *J. Appl. Spectr.*, **62**, No. 6: 1060 (1995); https://doi.org/10.1007/BF02606760
19. K. Wasa, M. Kitabatake, and H. Adachi, *Thin Film Materials Technology: — Sputtering of Compound Materials* (New York: Springer–William Andrew Inc Publishing: 2004).
20. O. M. Bordun, B. O. Bordun, I. J. Kukharskyy, I. I. Medvid, O. Ya. Mylyo, M. V. Partyka, and D. S. Leonov, *Nanosistemi, Nanomateriali, Nanotehnologii*, **17**, Iss. 1: 123 (2019); https://doi.org/10.15407/nnn.17.01.123
21. C. V. Thompson, *Sol. State Phys.*, **55**: 269 (2001); https://doi.org/10.1016/S0081-1947(01)80006-0
22. C. V. Thompson, *J. Appl. Phys.*, **58**: 763 (1985); https://doi.org/10.1063/1.336194
23. O. M. Bordun, B. O. Bordun, I. Yo. Kukharskyy, I. I. Medvid, I. I. Polovynko, Zh. Ya. Tsapovska, and D. S. Leonov, *Nanosistemi, Nanomateriali, Nanotehnologii*, **19**, Iss. 1: 159 (2021); https://doi.org/10.15407/nnn.19.01.159
24. J. E. Palmer, C. V. Thompson, and Henry L. Smith, *J. Appl. Phys.*, **62**, No. 6: 2492 (1987); https://dx.doi.org/10.1063/1.339460
25. O. M. Bordun, I. O. Bordun, I. M. Kofliuk, I. Yo. Kukharskyy, I. I. Medvid, Zh. Ya. Tsapovska, and D. S. Leonov, *Nanosistemi, Nanomateriali, Nanotehnologii*, **20**, Iss. 1: 91 (2021); https://doi.org/10.15407/nnn.20.01.091